Inorganic Chemistry

Article

pubs.acs.org/IC

# Luminescent Calix[4]arene-Based Metallogel Formed at Different Solvent Composition

Jaehyeon Park,[†] Ji Ha Lee,[†] Justyn Jaworski,[‡] Seiji Shinkai,[∥] and Jong Hwa Jung*[,†]

[†]Department of Chemistry & Research Institute of Natural Science, Gyeongsang National University, Jinju 660-701, Republic of Korea

[‡]Department of Chemical Engineering, Hanyang University, Seoul 133-791, Korea

[∥]Institute for Advanced Study, Kyushu University, Fukuoka 819-0395, Japan

Supporting Information

**ABSTRACT:** We have synthesized a calix[4]arene derivative (**1**) containing terpyridine and showed that gelation occurred in the presence of $Pt^{2+}$ in DMSO/$H_2O$ of varying compositions. Gelation was presumably mediated by the Pt−Pt and $\pi-\pi$ stacking interactions. The scanning electron microscopy image of the xerogel showed a spherical structure with diameter of 1.8−2.1 $\mu$m. Interestingly, the metallogel showed strong luminescence enhancement, which was dependent on the DMSO/$H_2O$ ratio of the solvent. We examined the effects of concentration, temperature, and time resolution on the luminescence emission of both the gel **1**-$Pt^{2+}$ and the sol **1**-$Pt^{2+}$. The luminescence lifetimes of the metallogel were particularly long, on the order of several microseconds. The luminescence lifetimes were also strongly dependent on the solvent composition. We also determined the thermodynamic parameters for the self-assembly of the gel by the Birks kinetic scheme. Furthermore, the rheological properties of the metallogels in the presence of more than 4.0 equiv of $Pt^{2+}$ were independent of the concentration of $Pt^{2+}$ applied.

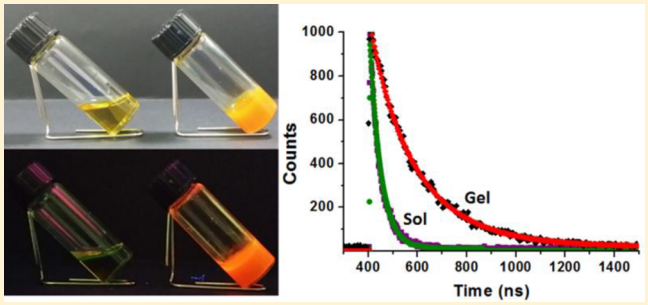


## INTRODUCTION

Recently, the generation of supramolecular gels from components ranging in size from small molecules to polymeric species has been realized by employing noncovalent interactions, which include hydrophobic interactions, $\pi-\pi$ stacking, hydrogen bonding, and even metal−ligand interactions.[1−8] The application of supramolecular gels to the field of material science has afforded benefits including information recording materials, drug releasing materials, and adaptive material.[9−12]

The utilization of metal−ligand coordination chemistry for the directed self-assembly of small molecules has opened a new branch of materials research. The diverse and unidirectional properties of metal−ligand interactions allow the formation of controllable and extended structures, thus establishing these interactions as the primary driving force in the construction of supermolecular structures. Depending on the metal centers, the coordination geometry, and the coordinating ligand, these metal complexes offer various functional properties, such as intriguing spectroscopic, catalytic, and redox properties among others.[13−15] The incorporation of metal centers into supramolecular gels may yield multifunctional metallogels that could not be achieved in organogels.

Research interest in square planar platinum(II) terpyridyl complexes has grown in recent years, as these coordination compounds have exciting luminescence and spectroscopic properties, in addition to their propensity for $\pi-\pi$ as well as metal−metal interactions.[16−22] Among these compounds, the striking changes in the color and luminescence enhancement of the organometallic alkynylplatinum(II) terpyridyl complexes are some of the most interesting from an applications perspective, since changes in their intermolecular interactions are easily caused by solvent, temperature, and other stimuli. Recently, Yam and other groups have reported that the sol−gel transition of alkynylplatinum(II) terpyridyl complexes afforded very distinctive changes in color.[21−23] Also, Yam's group demonstrated that the solvent composition could be used to control the supramolecular self-assembly of amphiphilic anionic platinum(II) pyridyl complexes[24] via $\pi-\pi$ stacking interactions and aggregation of Pt−Pt.

Furthermore, their luminescence lifetimes are on the order of nanoseconds. However, the effect of external stimuli on the luminescent properties of metallogels induced by $Pt^{2+}$ has been less well studied, particularly stimuli such as variation of solvent composition and the change of concentration of the ligand. In the present study, we used the framework of calix[4]arene for ligand attachment, since the calix[4]arene moiety has proven to be an effective core species for self-assembly. In addition, the multifunctional groups can easily allow the introduction of carboxyl functionalities for hydrogen-bonding and specific ligand groups as sites for coordination. In particular, the 1,3-alternate calix[4]arene moiety can form a coordinated polymer

**Received:** February 3, 2014
**Published:** July 10, 2014

   dx.doi.org/10.1021/ic500266f | *Inorg. Chem.* 2014, 53, 7181−7187

structure.[25−27] Herein, we describe the preparation of a terpyridine-appended calix[4]arene metallogel incorporating $Pt^{2+}$. We investigated its luminescence properties in various compositions of solvent, and we observed its luminescence emission as affected by concentration dependence, variation in temperature, and time-resolved luminescence emission.

## EXPERIMENTAL SECTION

**Instruments.** The NMR spectra for $^1H$ and $^{13}C$ NMR were measured using a Bruker ARX 300 apparatus. For the IR spectra, KBr pellets were formed, and the IR spectra were observed over the range 400−4000 $cm^{-1}$, with a Shimadzu FT-IR 8400S instrument. In addition, the mass spectra were observed using a JEOL JMS-700 mass spectrometer. A UV−visible (UV−vis) spectrophotometer (Thermo Evolution 600) was used to obtain the absorption spectra, and the fluorescence spectra were obtained using a RF-5301PC spectrophotometer, which was also used for the variable-temperature emission measurements. These measurements were obtained from a single-cell to control the working temperature in the range 25−90 °C. Gels were measured using a 0.50 mm path length quartz cuvette as well as a 4 mm path length quartz cuvette for emission measurements. The thermodynamic parameters were determined by a literature method reported previously.[28]

**Electron Microscopy.** A JEOL JEM-2010 transmission electron microscope operating at 200 kV was used for examining the samples using an accelerating voltage of 100 kV and operating at a 16 mm working distance. A field emission scanning electron microscope (Philips XL30 S FEG) was also used to observe the samples in which an accelerating voltage of 5−15 kV with an emission current of 10 $\mu$A was used. Prior to scanning electron microscopy (SEM) visualization, the metallogel was also freeze-dried under vacuum at −5 °C.

**Rheological Measurements.** Fresh Pt-terpyridine gels were analyzed for their rheological properties using a controlled stress rheometer (AR-2000ex, TA Instruments Ltd., New Castle, DE, USA). Throughout the experiments, a cone-type geometry of 40 mm diameter was used. By using a frequency of 0.1 rad $s^{-1}$, the dynamic oscillatory behavior was examined. In addition, the response was observed upon increased amplitude oscillations with up to 100% apparent strain on shear and having frequency sweeps at 25 °C (from 0.1 to 100 rad $s^{-1}$, respectively). Finally, the unidirectional shear was examined at 25 °C with a shear-rate regime between $10^{-1}$ and $10^3$ $s^{-1}$ using transient measurements in the mechanical spectroscopy routines.

**Fluorescence Lifetime Measurements.** By using a conventional laser system, the emission lifetimes were measured upon generation with an excitation source (420 nm output of a Spectra-Physics Quanta-Ray Q-switched GCR-150−10 pulsed Nd/YAG laser). The signals for the luminescence decay were obtained using a Hamamatsu R928 PMT, and the data was recorded on a Tektronix model TDS-620A (500 MHz, 2 GS/s) digital oscilloscope from which it was exponentially fit for analysis.

**Fluorescence Microscopy.** A Nikon microscope ECLIPSE 80i was used to record images with a 420 nm UV light excitation source. The emission spectra between 465 and 495 nm were obtained with 100× magnification. The samples for microscopy were formed by the drop-casting method on to a glass slide and allowing for slow evaporation.

**Typical Experimental Procedure for the Formation of Pt-Calix[4]arene-Based Gel 1.** Compound **1** (4 mg, 1.0 wt %) was added to DMSO (0.28 mL). $PtCl_2$ (0−6.0 equiv) was dissolved in a small volume of $H_2O$ (0.12 mL). Compound **1** dissolved in DMSO was mixed in the $Pt^{2+}$ solution. The sample was maintained at room temperature to form the gel.

**Synthesis of Compound 2.** *p-tert*-Butyl phenol (150 g, 1 mol) and NaOH (1.8 g, 45 mmol) was dissolved in 37% formaldehyde (100.7 g, 1.24 mol). The reaction mixture was refluxed at 120 °C for 12 h. After the solution was cooled to room temperature, $H_2O$ was removed in vacuo, and then, diphenyl ether (450 mL) and toluene (150 mL) were added. The reaction mixture was refluxed at 250 °C, again. The color of the reaction mixture changed to dark brown. Then, the crude product was recrystallized from ethyl acetate (300 mL) and was washed with acetic acid (100 mL) to give white crystalline solid **2** in 56.79% yield. mp 343 °C; IR (KBr pellet) 3176, 2958, 2866, 1603, 1482, 1361, 1242, 1200, 1042, 871, 816, 783; $^1H$ NMR (300 MHz, DMSO-$d_6$) $\delta$ ppm 10.36 (s, 4H), 7.07 (s, 8H), 3.52 (s, 4H), 1.23 (s, 36H); $^{13}C$ NMR (75 MHz DMSO-$d_6$) $\delta$ ppm 147.62, 143.63, 126.96, 125.74, 34.52, 33.1, 31.2; ESI-MS: calculated for $C_{44}H_{56}O_4$ $[M + H]^+$ 649.42, found 649.35; anal. calcd for $C_{44}H_{56}O_4$: C, 81.44; H, 8.70. Found: C, 81.75; H, 8.59.

**Synthesis of Compound 3.** A suspension of $AlCl_3$ (24 g, 180 mmol) and toluene (150 mL) was stirred in a 1 L three-necked round-bottom flask. The contents of the flask were poured into a suspension of compound **2** (20 g, 30.8 mmol), $CH_2Cl_2$ (200 mL), and toluene (50 mL). After the reaction mixture was stirred for 0.5 h, $CH_2Cl_2$ (100 mL) and 10% aqueous HCl (400 mL) solution were added to the reaction mixture in an ice bath. Finally, the reaction mixture was extracted with $CH_2Cl_2$ (3 × 200 mL), washed twice with water, and dried over anhydrous $MgSO_4$, and the solvent was removed in vacuo. The crude product was recrystallized from $CH_2Cl_2$/ethyl ether (1:30, v/v) to give a beige crystalline solid **3** in 66.5% yield (8.7 g). mp 315 °C; IR (KBr pellet) 3160, 2935, 2870, 1594, 1465, 1448, 1244, 752; $^1H$ NMR (300 MHz, DMSO-$d_6$) $\delta$ ppm 9.76 (br, 4H), 7.16 (d, 8H), 6.66 (t, 4H), 3.89 (s, 4H); $^{13}C$ NMR (75 MHz DMSO-$d_6$) $\delta$ ppm 149.8, 129.2, 129.0, 121.7, 31.1; ESI-MS: calculated for $C_{28}H_{24}O_4$ $[M + H]^+$ 425.17, found 425.28; anal. calcd for $C_{28}H_{24}O_4$: C, 79.22; H, 5.70. Found: C, 79.31; H, 5.65.

**Synthesis of Compound 4.** Compound **3** (5.00 g, 11.78 mmol) and $Cs_2CO_3$ (38.4 g, 11.78 mmol) were suspended in dry acetone (250 mL) and added to the solution of ethyl 2-bromoacetate (11.81 g, 70.68 mmol) in dry acetone (25 mL). The reaction mixture was refluxed for an additional 4 h. After cooling to room temperature, the salt was filtered, and the solvent (acetone) was removed in vacuo. To the resulting pale yellow oil, 10% aqueous HCl (100 mL) solution and $CH_2Cl_2$ (100 mL) were added, and the organic layer was separated, washed twice with water, and dried over anhydrous $MgSO_4$, and the solvent was removed in vacuo. The crude product was recrystallized from $CH_2Cl_2$/*n*-hexane (1:30, v/v) to give a white crystalline solid **4** in 45.5% yield (4.12 g). mp 118 °C; IR (KBr pellet) 3062, 2980, 2938, 1758, 1453, 1180, 1095, 1060, 769; $^1H$ NMR (300 MHz, DMSO-$d_6$) $\delta$ ppm 7.07 (d, 8H), 6.65 (t, 4H), 4.17 (q, 8H), 3.96 (s, 8H), 3.79 (s, 8H), 1.23 (t, 12H); $^{13}C$ NMR (75 MHz DMSO-$d_6$) $\delta$ ppm 169.9, 158.2, 133.8, 130.6, 122.7, 69.8, 60.7, 35.7, 14.5; ESI-MS: calculated for $C_{44}H_{48}O_{12}$ $[M + Na]^+$ 791.30, found 791.25; anal. calcd for $C_{44}H_{48}O_{12}$: C, 68.74; H, 6.29. Found: C, 68.68; H, 6.34.

**Synthesis of Compound 5.** A solution of compound **4** (2 g, 2.6 mmol) in the mixture of THF (40 mL) and EtOH (40 mL) was heated to reflux temperature. The reaction mixture was then added to aqueous KOH (1 mL, 26 mmol). After refluxing for 4 h, the organic solvents were removed in vacuo, and water (10 mL) was added. The remaining aqueous solution was acidified to pH 1 by addition of 6 N HCl. The resulting precipitate was filtered and washed with water. The precipitation was dried under vacuum to give compound **5** as a white solid in 79.7% yield (1.36 g,). mp 303 °C; IR (KBr pellet) 3448, 3015, 2925, 1731, 1460, 1356, 1322, 1195, 1058, 767; $^1H$ NMR (300 MHz, DMSO-$d_6$) $\delta$ ppm 12.48 (br, 4H), 7.12 (d, 8H), 6.69 (t, 4H), 4.12 (s, 8H), 3.83 (s, 8H); $^{13}C$ NMR (75 MHz DMSO-$d_6$) $\delta$ ppm 169.5, 154.4, 134.7, 124.1, 122.7, 72.5, 34.1; ESI-MS: calculated for $C_{36}H_{32}O_{12}$ $[M + K]^+$ 695.15, $C_{36}H_{32}O_{12}$ $[M + Na]^+$ 679.17, found 695.25, 679.50; anal. calcd for $C_{36}H_{32}O_{12}$: C, 65.85; H, 4.91. Found: C, 66.21; H, 4.97.

**Synthesis of Compound 8.** 4′-Chloro-[2,2′,6′,2″]terpyridine (1 g, 3.73 mmol) (**7**) was suspended in 1,3-propane diamine (8.305 g, 111.9 mmol). Upon heating, the solution became yellow. The reaction mixture was then heated under reflux conditions (120 °C) overnight. After cooling to room temperature, $H_2O$ (50 mL) was added, and a white precipitate was formed. After filtration, the solid was washed with $H_2O$. The solid was dissolved in $CH_2Cl_2$ and extracted twice with $H_2O$. The organic layers were combined, dried over anhydrous $Na_2SO_4$, and filtered, and the solvent was removed under reduced pressure to yield a white solid in 88.67% yield (1.01 g). mp 148 °C; IR


dx.doi.org/10.1021/ic500266f | Inorg. Chem. 2014, 53, 7181−7187

**Scheme 1. Schematic Synthetic Route of Ligand 1**

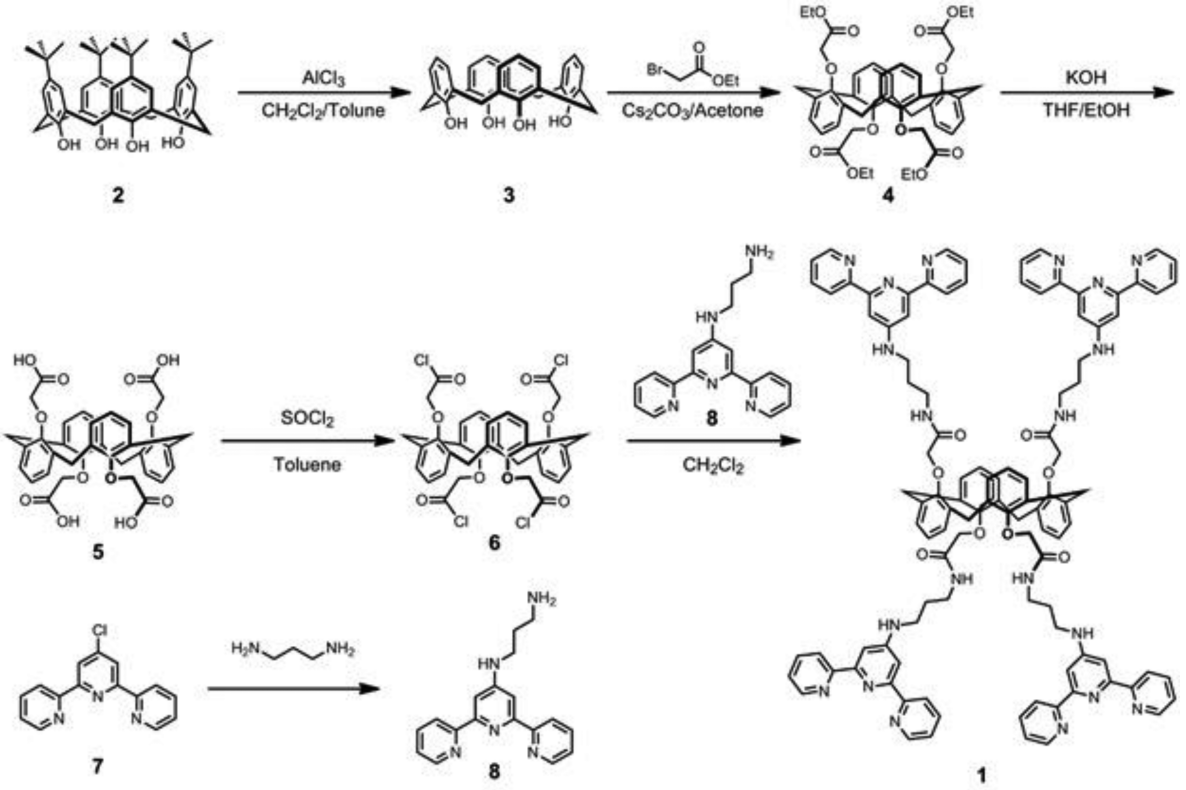


(KBr pellet) 3410, 3380, 3230, 3056, 3010, 2919, 2860, 1605, 1582, 1566, 1511, 1465, 1457, 1446, 1237, 1111, 1090, 1043, 990, 858, 835, 793, 743, 656; $^1$H NMR (300 MHz, MeOD) $\delta$ ppm 8.62 (m, 2H), 8.50 (d, 2H), 7.95 (m, 2H), 7.52 (s, 2H), 7.44 (m, 2H), 3.38 (t, 2H), 2.82 (m, 2H), 1.88 (q, 2H); $^{13}$C NMR (75 MHz MeOD) $\delta$ ppm 156.5, 155.7, 155.1, 149.2 135.8, 124.2, 121.3, 104.5, 41.6, 40.8, 32.3; ESI-MS: calculated for $C_{18}H_{19}N_5$ $[M + H]^+$ 306.17, found 306.25; anal. calcd for $C_{18}H_{19}N_5$: C, 70.80; H, 6.27; N, 22.93. Found: C, 70.74; H, 6.23; N, 22.88.

**Synthesis of Compound 1.** To a suspension of compound **5** (0.2 g, 0.30 mmol) in toluene (20 mL) was added $SOCl_2$ (0.265 mL, 3.65 mmol). The reaction mixture was refluxed for 4 h and was cooled to room temperature. The solvent and unreacted $SOCl_2$ were removed to give compound **6**. Compound **6** without purification was dissolved in $CH_2Cl_2$ (10 mL). Then, the solution of compound **8** (0.465 g, 15.2 mmol) in $CH_2Cl_2$ (10 mL) and TEA (0.5 mL) was added and stirred for 12 h. After filtration of the reaction mixture, the solvent was removed in vacuo. The crude product was dissolved in $CH_2Cl_2$, washed twice with water, and dried over anhydrous $MgSO_4$, and the solvent was removed in vacuo. The crude product was recrystallized in $CH_2Cl_2$/ethyl ether (1:30, v/v) to give a withe solid **1** as a final product in 70.0% yield (0.38 g). mp 207 °C; IR (KBr pellet) 3397, 3245, 3055, 3010, 2928, 1647, 1605, 1585, 1565, 1461, 1445, 1405, 1355, 1246, 1225, 1199, 1092, 1042, 996, 984, 858, 792, 745, 622; $^1$H NMR (300 MHz, DMSO-$d_6$) $\delta$ ppm 8.64 (d, $J$ = 4.68 Hz, 8H), 8.53 (d, $J$ = 7.61 Hz, 8H), 7.91 (m, 8H), 7.67 (s, 8H), 7.40 (m, 8H), 7.03 (d, $J$ = 7.68 Hz, 8H), 6.71 (t, $J$ = 7.40 Hz, 4H), 6.59 (t, $J$ = 5.43 Hz, 4H), 3.83 (s, 16H), 3.32 (br, 4H), 3.17 (m, 16H), 1.74 (m, 8H); $^{13}$C NMR (125 MHz, DMSO-$d_6$) $\delta$ ppm 167.58, 158.48, 157.22, 155.48, 148.55, 136.33, 134.85, 123.64, 122.52, 120.23, 106.54, 67.58, 40.58, 38.12, 33.54, 28.15; ESI-MS: calculated for $C_{108}H_{100}N_{20}O_8$ $[M + H]^+$ 1805.81, $[M + 2H]^{2+}$ 903.91, $[M + 3H]^{3+}$ 602.94, $[M + 4H]^{4+}$ 452.46, found 1806.33, 903.75, 602.92, 452.58; anal. calcd for $C_{108}H_{100}N_{20}O_8$: C, 71.82; H, 5.58; N, 15.51. Found: C, 71.72; H, 5.54; N, 15.56.

**Synthesis of 1-[PtCl]$_4$Cl$_4$.** Compound **1** (0.2 g, 0.11 mmol) was allowed to react with $PtCl_2$ (0.118 g, 0.44 mmol) in 5 mL of DMSO with stirring at 100 °C for 2 days. After cooling to room temperature, the yellowish solution was concentrated under vacuum. Acetone (10 mL) was added to the mixture. The orange precipitate was collected, washed with acetone, and dried under vacuum (0.21 g; yield 73%). mp 220 °C; IR (KBr pellet) 3393, 3247, 3080, 2932, 1625, 1541, 1508, 1457, 1363, 1245, 1193, 1094, 1034, 782, 623; $^1$H NMR (300 MHz, DMSO-$d_6$, $T$ = 373 K) $\delta$ ppm 8.70 (d, $J$ = 5.58 Hz, 8H), 8.47 (d, $J$ = 4.98 Hz, 8H), 8.30 (m, 8H), 7.80 (m, 8H), 7.42 (s, 8H), 7.14 (d, $J$ = 7.60 Hz, 8H), 6.82 (m, 4H), 6.74 (m, 4H), 4.05 (s, 8H), 4.00 (m, 4H), 3.95 (s, 8H), 3.47 (m, 8H), 3.27 (m, 8H), 1.88 (m, 8H); $^{13}$C NMR (125 MHz, DMSO-$d_6$, $T$ = 373 K) $\delta$ ppm 168.22, 159.23, 156.88, 154.28, 143.83, 142.26, 130.71, 126.24, 125.58, 125.22, 124.52, 106.21, 67.7, 40.78, 38.25, 32.45, 28.12; ESI-MS: calculated for $[C_{108}Cl_4H_{100}N_{20}O_8Pt_4Cl_4]^{4+}$ 681.88, found 681.81; anal. calcd for $C_{108}Cl_8H_{100}N_{20}O_8Pt_4$: C, 47.55; H, 3.69; N, 10.27. Found C, 47.47; H, 3.70; N, 10.28.

## RESULTS AND DISCUSSION

Calix[4]arene-based ligand **1** was synthesized in six steps (Scheme 1). The starting compound **2** was prepared by a modified literature method. Compound **2** was treated with $AlCl_3$ in DCM/toluene to remove the *tert*-butyl group. Compound **3** was reacted with ethyl 2-bromoacetate in the presence of $Cs_2CO_3$ to obtain compound **4** in acetone. After chlorination of compound **5**, the coupling of compounds **6** and **8** synthesized from 4′-chloro-2,2′:6′,2″-terpyridine was performed in methylene chloride in the presence of triethylamine to produce desired ligand **1** in 70% yield, as confirmed by $^1$H and $^{13}$C NMR, mass spectrometry (MS), and elemental analysis.

A metallogel based on **1** was prepared by dissolving 1.0 wt % of **1** in a mixture of DMSO (1:1 v/v) and with one of the following solvents: chloroform, methylene chloride, toluene, methanol, ethanol, ethyl acetate, acetonitrile, tetrahydrofuran, acetone, and water. To this solution was added 4.0 equiv of $Pt^{2+}$


dx.doi.org/10.1021/ic500266f | Inorg. Chem. 2014, 53, 7181−7187

with 4.0. The following samples were then set, undisturbed, for 1 week. As shown in Figure S1 and Table S1 (Supporting Information), ligand **1** after exposure to $Pt^{2+}$ gelated in a mixture of water and DMSO (1:1 v/v). In addition, the gelation ability of ligand **1** was tested in a mixture of $H_2O$/DMSO (7:3 v/v) in concentrations varying from 0 to 4.0 equiv with respect to the ligand concentration. In a gelation test of **1** from 0 to 4.0 equiv of $Pt^{2+}$ with $H_2O$/DMSO of composition (7:3 v/v), we observed that the critical gel concentration (CGC) of metallogel **1** with $Pt^{2+}$ (4.0 equiv) was 2.1 ± 0.2 mM (Figure 1). Opaque gel **1** was obtained with 4.0 equiv of $Pt^{2+}$ (Figure 1). On the other hand, calix[4]arene-based ligand **1** did not form a gel with less than 4.0 equiv of $Pt^{2+}$. The tetra-terpyridine group of **1** formed a complex with four $Pt^{2+}$ ions to induce gel formation, which had a square planar structure. The molecular weight of the **1**-$Pt^{2+}$ complex was measured by electrospray ionization (ESI) MS. As shown in Figure S2 (Supporting Information), evidence for the 1:4 complex is found in the ESI mass spectrum of the **1**-$[PtCl]_4^{4+}$ complex (681.84 $m/e$).

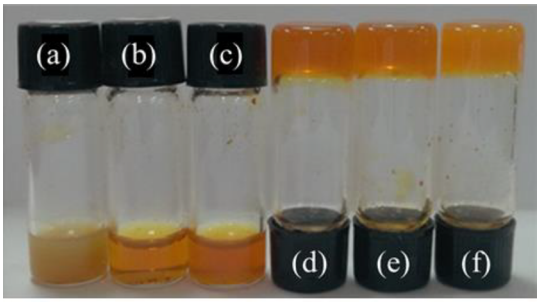


**Figure 1.** Photograph of metallogel **1** with (a) 1.0 equiv, (b) 2.0 equiv, (c) 3.0 equiv, (d) 4.0 equiv, (e) 5.0 equiv, and (f) 6.0 equiv of $Pt^{2+}$ in $H_2O$/DMSO (7:3 v/v).

The morphology of xerogel **1** obtained with $Pt^{2+}$ (4.0 equiv) was investigated by SEM, transmission electron microscopy (TEM), and fluorescence microscopy. The SEM image of $Pt^{2+}$ metallogel **1** clearly displayed a spherical structure with diameters of 1.8−2.1 $\mu$m (Figure 2). Fluorescence images of metallogel **1** emitted a strong red color upon excitation at 420 nm. In particular, we performed elemental mapping by energy dispersive X-ray spectroscopy (EDX) coupled with TEM observation. The metallogel contained carbon, oxygen, nitrogen, and platinum components (Figure 2C). These findings strongly support the view that **1** formed a complex with $Pt^{2+}$ to induce gelation.

Since ligand **1** could gelate a mixture of $H_2O$/DMSO in the presence of 4.0 equiv of $Pt^{2+}$, quantitative luminescence properties of metallogel **1**-$[PtCl]_4^{4+}$ were measured. In various solutions of $H_2O$/DMSO (1:9, 2:8, 8:2, 9:1 v/v), **1**-$[PtCl]_4^{4+}$ was weakly fluorescent (Figure 3A; a, b), but upon gelation with $H_2O$/DMSO (3:7−7:3 v/v), it emitted strong red fluorescence under UV light (Figure 3A; c−g). The fluorescence emission properties as well as the absorption spectra of sol **1**-$[PtCl]_4^{4+}$ and metallogel **1**-$[PtCl]_4^{4+}$ were observed. The absorption band of metallogel **1** appeared at 420 nm (Figure S3, Supporting Information), which was assigned as $d\pi(Pt) \rightarrow \pi^*(tpy)$ metal-to-ligand charge transfer (MLCT).[29−33] The emission spectra of metallogel **1** with different contents of $H_2O$/DMSO were recorded upon excitation at 420 nm (Figure 3B). In the absence of $H_2O$, an emission band centered at 570 nm was observed. The band intensity dropped dramatically for higher proportions of $H_2O$. Simultaneously, a new emission band appeared at 660 nm, which originated from an excimer emission that is believed to be attributed to the formation of aggregate species. This emission is attributed to a MLCT excited state that involves the terpyridine $\pi^*$ as the lowest unoccupied molecular orbital. Pt−Pt interactions are expected to affect the metal-based highest occupied molecular orbital of metallogel **1**-$[Pt^{2+}]_4$, thereby corresponding to a $d\sigma^*$ function formed by overlapping $d_z^2$ orbitals that are formally antibonding in respect to the Pt−Pt interaction. As a result of the metal−metal interaction, the

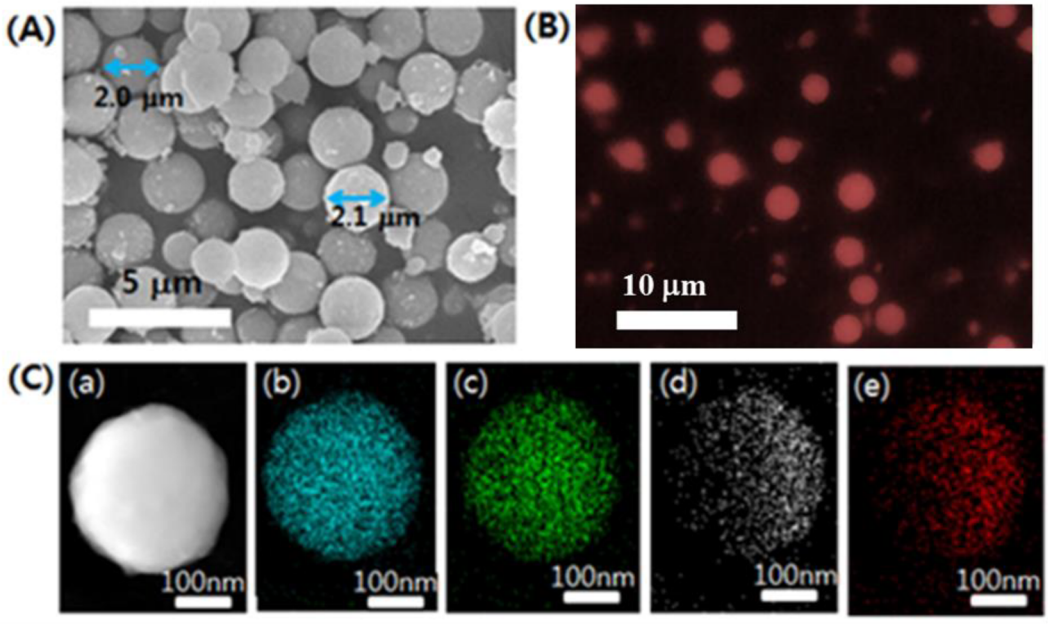


**Figure 2.** (A) SEM and (B) fluorescence microscopy images of metallogel **1** (1.0 wt %) with $Pt^{2+}$ (4.0 equiv) in $H_2O$/DMSO (7:3 v/v). (C) EDX mapping of metallogel **1** by TEM observation; (a) bright-field image, (b) platinum, (c) carbon, (d) oxygen, and (e) nitrogen components.


dx.doi.org/10.1021/ic500266f | Inorg. Chem. 2014, 53, 7181−7187

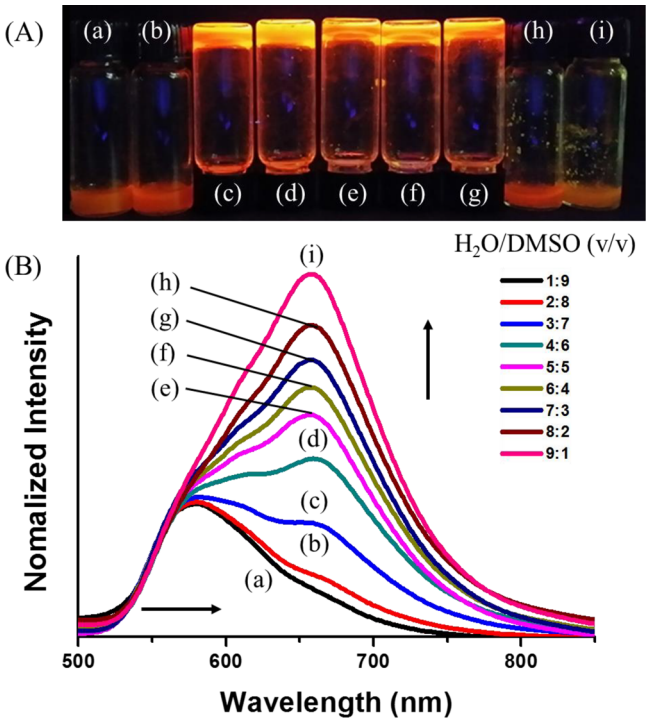


**Figure 3.** (A) Photograph of gel **1**-$[PtCl]_4^{4+}$ (1.0 wt %) under UV light at different solvent compositions of $H_2O$/DMSO; (a) 1:9, (b) 2:8, (c) 3:7, (d) 4:6, (e) 5:5, (f) 6:4, (g) 7:3, (h) 8:2, and (i) 9:1. (B) Emission spectra of **1**-$[PtCl]_4^{4+}$ at different solvent compositions of $H_2O$/DMSO; (a) 1:9, (b) 2:8, (c) 3:7, (d) 4:6, (e) 5:5, (f) 6:4, (g) 7:3, (h) 8:2, and (i) 9:1 at 25 °C. The emission spectra were normalized at 570 nm.

emissive state of metallogel **1**-$[Pt^{2+}]_4$ is thus designated as $^3$MMLCT (triplet metal–metal-to-ligand charge transfer).[29−33] The higher emission of metallogel **1** formed in the presence of $Pt^{2+}$ with increasing $H_2O$ content is due to stronger Pt–Pt and $\pi-\pi$ stacking interactions than those formed in DMSO.[29−33]

We also studied $^1$H NMR spectra of metallogel **1** with $Pt^{2+}$ (4.0 equiv) by increases in temperature (Figure S4, Supporting Information). The protons of the terpyridine moieties were shifted to a lower magnetic field by increasing temperature. In addition, the proton peaks of the terpyridine moieties became sharper at increasing temperature. These results indicated that ligand **1** with $Pt^{2+}$ forms a self-assembled structure by intermolecular interactions between the terpyridine groups as well as $Pt^{2+}$ at low temperature but dissociated at high temperatures. Figure S5 (Supporting Information) shows the proposed structure of metallogel **1** with $Pt^{2+}$ based on fluorescence, mass, and NMR observations. Metallogel **1** with $Pt^{2+}$ could be formed through a self-assembled network structure by intermolecular interactions such as $\pi-\pi$ stacking and MLCT. In particular, the distance between the terpyridine and the terpyridine groups involved in the intermolecular interactions such as $\pi-\pi$ stacking as well as the Pt–Pt distances were in the range 3.3–3.8 Å.[22,34]

Figure 4A shows the changes in the emission spectra of different concentrations of **1**-$[PtCl]_4^{4+}$ in $H_2O$/DMSO (3:7 v/v), which is the sol phase. At concentrations decreasing from $1.0 \times 10^{-4}$ to $1.0 \times 10^{-6}$ M at 298 K, the emission band at 660 nm decreased in intensity with an associated appearance of a new emission band at 570 nm. The luminescence spectra of the dilute samples ([**1**-$[PtCl]_4^{4+}$] = $1.0 \times 10^{-4}$ M) were also observed by varying the temperature (Figure 4B). By elevating the temperature of the dilute solution of **1**-$[PtCl]_4^{4+}$ from 313 to 353 K, we could also observe a decrease in the 660 nm emission band, while the band at 570 nm increased in intensity upon excitation at $\lambda$ = 420 nm, with an isoemissive point at 620 nm (Figure 4B). Given that the emission band at 660 nm depends on temperature as well as concentration, we propose an excimer emission originating from the formation of an aggregate species in $H_2O$/DMSO (3:7 v/v),[28] since such a decrease in temperature or increase in concentration is known to lead to aggregate formation.[32] While excimer emissions at high concentration are proposed attributable to the dependence of the emission band with respect to concentration, Birks kinetic scheme was used to describe temperature-dependent changes in the ratio of aggregate to monomer.[35−38] The Stevens–Ban plot[39] of $\ln(I_{agg}/I_{mono})$ versus $1/T$ in $H_2O$/DMSO (3:7 v/v) yielded a positive slope (Figure 4C), which has been suggestive of a high-temperature system limit ($I_{agg}$ and $I_{mono}$ are the emission intensities at 660 and 570 nm, respectively). Below this limit, an excimer binding enthalpy ($\Delta H$) of $-26.14 \pm 1.20$ kJ mol$^{-1}$ was found from the positive slope of the Stevens–Ban plot (Figure 4C) of **1**-$[PtCl]_4^{4+}$ ($2.7 \times 10^{-6}$ M) in $H_2O$/DMSO.[25,26] A corresponding binding entropy ($\Delta S$) of $-26.36$ J mol$^{-1}$ K$^{-1}$ was observed from the $y$ intercept of the Stevens–Ban plot and the negative slope of the plot of $I_{agg}$ against $I_{mono}$. The Gibbs free energy change ($\Delta G$) of the excimer formation was calculated to be $-18.05$ kJ mol$^{-1}$.[28,40,41]

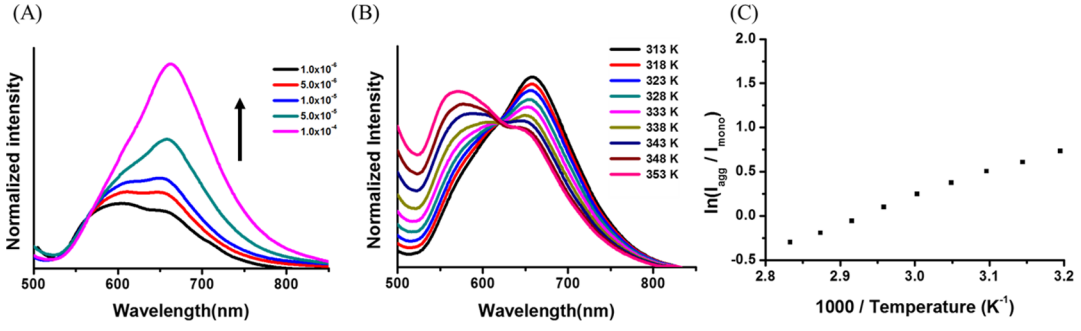


**Figure 4.** (A) Emission spectra of different concentrations of **1**-$[PtCl]_4^{4+}$ ($1.0 \times 10^{-6}$ to $1.0 \times 10^{-4}$) at $H_2O$/DMSO (3:7 v/v). (B) Emission spectra of **1**-$[PtCl]_4^{4+}$ at different temperatures (increasing from 313 to 353 K). (C) Corresponding Stevens–Ban plot of $\ln(I_{agg}/I_{mono})$ vs $1/T$ ($I_{agg}$ and $I_{mono}$ are the emission intensities at 660 and 570 nm at corresponding temperatures). Inset: corresponding plot of $I_{agg}/I_{mono}$. The emission spectra in (A) were normalized at 570 nm.


dx.doi.org/10.1021/ic500266f | Inorg. Chem. 2014, 53, 7181−7187

To better identify the excited-state behavior of metallogel **1** with $Pt^{2+}$, we conducted a time-resolved emission study of metallogel **1** with $Pt^{2+}$ using various concentrations of **1** (Figure 5). In the sol state, the luminescence lifetimes were found to be

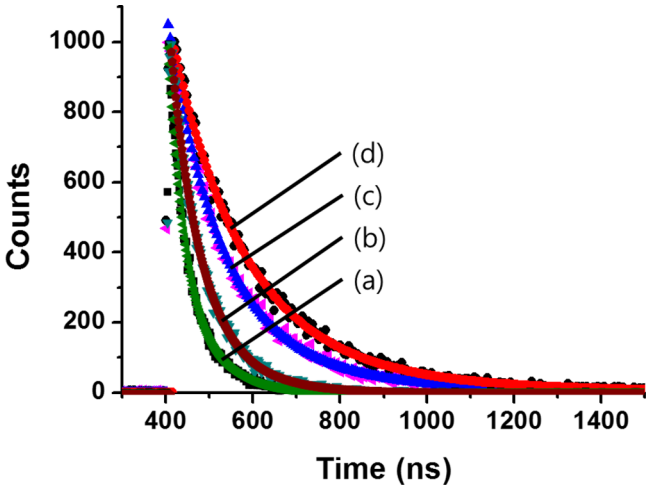


**Figure 5.** Emission decay curves of (a) sol **1**-$[PtCl]_4^{4+}$ (0.3 wt %) and metallogel **1**-$[PtCl]_4^{4+}$ (b) 0.5 wt %, (c) 0.7 wt %, and (d) 1.0 wt % obtained from $H_2O$/DMSO (3:7 v/v).

**Table 1. Luminescence Lifetimes of 1-$[PtCl]_4^{4+}$ at Different Concentrations in $H_2O$/DMSO (7:3 v/v)**

| conc of **1**-$[PtCl]_4^{4+}$ | $\tau_1$ | $\tau_2$ | phase |
|---|---|---|---|
| 0.3 wt % | 71.22 ns | 199.57 ns | sol |
| 0.5 wt % | 82.39 ns | 201.25 ns | gel |
| 0.7 wt % | 99.75 ns | 219.15 ns | gel |
| 1.0 wt % | 143.20 ns | 250.90 ns | gel |

71.22 and 199.57 ns (Table 1), much longer times than those reported in the literature.[28,42] In general, the luminescence lifetimes of nanomaterials induced with platinum ion are on the order of nanoseconds.[36,39] Therefore, the luminescence properties of **1** with $Pt^{2+}$ in the sol phase are unique. The long lifetimes of **1** with $Pt^{2+}$ are due to the existence of aggregation in the sol state. The biexponential luminescence decay may be due to aggregate formation in the sol state. At 0.5 wt % of **1** in the gel state, both the lifetimes, termed the $\tau_1$ and $\tau_2$ values, were slightly longer than those observed with 0.3 wt % of **1** in the sol state. An increase in the concentration of metallogel **1** (1.0 wt %) led to further increases of $\tau_1$ (143.20 ns) and $\tau_2$ (250.90 ns) values. On the other hand, the luminescence lifetimes of the solid **1** in the presence of $Pt^{2+}$ obtained with $H_2O$/DMSO (7:3 v/v) were found to be 79.82 and 205.32 ns for $\tau_1$ and $\tau_2$, respectively. In the gel state, the $\pi-\pi$ stacking interaction between the terpyridine and tertpyridine moieties was relatively weaker than those of the solid self-assemblies because the solvent molecules were located between the gelator molecules. Therefore, the emission in the gel state increased with increasing concentration of **1**.

We also investigated the time-resolved emission of metallogel **1**-$[PtCl]_4^{4+}$ with different ratios of $H_2O$/DMSO (Table 2 and Figure S6, Supporting Information). The luminescence lifetimes of the metallogel obtained with $H_2O$/DMSO (7:3 v/v) were found to be 143.20 and 250.90 ns for $\tau_1$ and $\tau_2$,

**Table 2. Luminescence Lifetimes of 1-$[PtCl]_4^{4+}$ at Different Solvent Compositions**

| $H_2O$/DMSO (v/v) | $\tau_1$ | $\tau_2$ | phase |
|---|---|---|---|
| 7:3 | 143.20 ns | 250.90 ns | gel |
| 5:5 | 109.90 ns | 210.12 ns | gel |
| 3:7 | 90.05 ns | 185.20 ns | gel |
| 0:10 | 25.16 ns | 95.25 ns | sol |

respectively. An increase of DMSO content led to shortening the $\tau_1$ and $\tau_2$ values. At $H_2O$/DMSO (3:7 v/v), we observed the shortest luminescence lifetime of metallogel **1**-$[PtCl]_4^{4+}$. The largest fluorescence intensity from gels prepared from $H_2O$/DMSO (7:3 v/v) had longest lifetime, because the strength of gel formation in $H_2O$/DMSO (7:3 v/v) was strongest due to intermolecular interactions such as MLCT and $\pi-\pi$ stacking. On the other hand, sol **1** with $Pt^{2+}$ in DMSO was weakly emissive. Thus, the lifetimes of solution **1** with $Pt^{2+}$ were 25.16 ns for $\tau_1$ and 95.25 ns for $\tau_2$.

The storage and loss moduli ($G'$ and $G''$, respectively) were obtained from rheology to offer a means for assessing the behavior of the metallogel under mechanical stress. The criteria of frequency independence of the dynamic storage modulus and also that the storage modulus should be an order of magnitude higher than the loss modulus must be met for a metallogel. We examined the dynamic strain sweep in order to find the appropriate conditions for the dynamic frequency sweep of the metallogel at different concentrations of $Pt^{2+}$. Figure S7A (Supporting Information) illustrates that $G'$ and $G''$ were almost constant with the increase of frequency from 0.1 to 100 rad $s^{-1}$. In addition, $G'$ is almost 5−7 times larger than $G''$ over the entire range (0.1−100 rad $s^{-1}$), suggesting that the metallogel is moderately tolerant to external force. As shown in Figure S7B (Supporting Information), the storage modulus ($G'$) and the loss modulus ($G''$) exhibited a weak dependence from 0.1% to 1.0% of strain (with $G'$ dominating $G''$). The observation of these met criteria indicates the sample as a metallogel. Both the storage modulus and the loss modulus of the metallogel in the presence of 4.0 equiv of $Pt^{2+}$ were similar to the metallogels in the presence of 5.0 and 6.0 equiv of $Pt^{2+}$. This suggests that the metallogel was almost completely formed and stabilized in the presence of 4.0 equiv of $Pt^{2+}$. The dynamic frequency sweep was used to study the metallogel after the strain amplitude was set to 0.01% (which is in the region of linear response for the strain amplitude). In addition, time-dependent oscillation measurements revealed the gelation processes of metallogels **1** with $Pt^{2+}$ (Figure S7C, Supporting Information). A quick increase in the storage modulus and loss modulus were both observed at the initial stage of the time sweep. A long, slow approach to a final pseudoequilibrium plateau was then found to occur. The final value of the storage modulus as the end of the experiment was almost 1 order of magnitude higher than that of the loss modulus.

## ■ CONCLUSIONS

In conclusion, calix[4]arene containing the terpyridine group in the presence of $Pt^{2+}$ formed a gel in solutions of various $H_2O$/DMSO compositions. Photophysical studies confirmed that the metallogel exhibited typical Pt−Pt and $\pi-\pi$ stacking interactions that gave rise to strong luminescence behavior. The metallogel showed a significant luminescence enhancement having a long lifetime by comparison to the sol. From the Birks kinetic scheme, we determined the values for the binding


dx.doi.org/10.1021/ic500266f | Inorg. Chem. 2014, 53, 7181−7187

enthalpy ($\Delta H$), binding entropy ($\Delta S$), and Gibbs free energy change ($\Delta G$) of the excimer. The dependence of concentration and temperature on luminescence suggested that enhancement was likely ascribed to the restricted molecular geometry being in favor of aggregate formation in the gel state. The luminescence lifetimes of the metallogel were also dependent on solvent composition. The rheological properties of the metallogel were independent of the concentration of $Pt^{2+}$. The results of this work provide an emphasis on the validity of ligand design making use of metal-binding components in realizing metallogel systems with versatile properties. We anticipate that this may help open the way for a range of responsive soft materials.

## ■ ASSOCIATED CONTENT

### Supporting Information

Information on gelation test of ligand **1**; photographs of ligand **1** with $Pt^{2+}$ in different solvents; ESI mass spectra, UV−vis absorption spectra, and $^1H$ NMR spectra; proposed structure of metallogel **1** with $Pt^{2+}$; emission decay curves; and dynamic oscillatory and steady-shear measurements. This material is available free of charge via the Internet at http://pubs.acs.org.

## ■ AUTHOR INFORMATION


### Corresponding Author

*E-mail: jonghwa@gnu.ac.kr; fax: +82-55-758-6027.


### Notes

The authors declare no competing financial interest.

## ■ ACKNOWLEDGMENTS

This work was supported by a grant from the NRF (2012002547, 2012R1A4A1027750, and 2014M2B2A9030338) supported from the Ministry of Education, Science and Technology, Korea. In addition, this work was partially supported by a grant from the Next-Generation BioGreen 21 Program (SSAC, grant no.: PJ009041022012), Rural Development Administration, Korea.

## ■ REFERENCES


(1) Fages, F. *Angew. Chem., Int. Ed.* **2006**, *45*, 1680−1682.
(2) Xing, B.; Choi, M.-F.; Xu, B. *Chem.—Eur. J.* **2002**, *8*, 5028−5032.
(3) Dastidar, P. *Chem. Soc. Rev.* **2008**, *37*, 2699−2715.
(4) Abdallah, D. J.; Weiss, R. G. *Adv. Mater.* **2000**, *12*, 1237−1247.
(5) Goh, C. Y.; Becker, T.; Brown, D. H.; Skelton, B. W.; Jones, F.; Mocerino, M.; Ogden, M. I. *Chem. Commun.* **2011**, *47*, 6057−6059.
(6) Becker, T.; Yong Goh, C.; Jones, F.; McIldowie, M. J.; Mocerino, M.; Ogden, M. I. *Chem. Commun.* **2008**, 3900−3902.
(7) Xing, B.; Choi, M.-F.; Xu, B. A. *Chem. Commun.* **2002**, 362−363.
(8) Foster, J. A.; Steed, J. W. *Angew. Chem., Int. Ed.* **2010**, *49*, 6718−6724.
(9) Sangeetha, N. M.; Maitra, U. *Chem. Soc. Rev.* **2005**, *34*, 821−836.
(10) Piepenbrock, M. O.; Lloyd, G. O.; Clarke, N.; Steed, J. W. *Chem. Rev.* **2010**, *110*, 1960−2004.
(11) Hirst, A. R.; Escuder, B.; Miravet, J. F.; Smith, D. K. *Angew. Chem., Int. Ed.* **2008**, *47*, 8002−8018.
(12) Banerjee, S.; Das, R. K.; Maitra, U. *J. Mater. Chem.* **2009**, *19*, 6649−6687.
(13) Tam, A. Y.; Yam, V. W. W. *Chem. Soc. Rev.* **2013**, *42*, 1540−1567.
(14) Zhang, J.; Su, C. Y. *Coord. Chem. Rev.* **2013**, *257*, 1373−1408.
(15) Weng, W.; Beck, J. B.; Jamieson, A. M.; Rowan, S. J. *J. Am. Chem. Soc.* **2006**, *128*, 11663−11672.
(16) Wong, K. M. C.; Yam, V. W. W. *Coord. Chem. Rev.* **2007**, *251*, 2477−2488.
(17) Williams, J. A. Photochemistry and Photophysics of Coordination Compounds: Platinum. In *Photochemistry and Photophysics of Coordination Compounds II*; Balzani, V., Campagna, S., Eds.; Springer: Berlin, Germany, 2007; pp 205−268.
(18) Lai, S. W.; Che, C. M. Luminescent Cyclometalated Diimine Platinum(II) Complexes: Photophysical Studies and Applications. In *Transition Metal and Rare Earth Compounds*; Yersin, H., Ed.; Springer: Berlin, Germany, 2004; pp 27−63.
(19) McMillin, D. R.; Moore, J. J. *Coord. Chem. Rev.* **2002**, *229*, 113−121.
(20) Pettijohn, C. N.; Jochnowitz, E. B.; Chuong, B.; Nagle, J. K.; Vogler, A. *Coord. Chem. Rev.* **1998**, *171*, 85−92.
(21) Houlding, V. H.; Miskowski, V. M. *Coord. Chem. Rev.* **1991**, *111*, 145−152.
(22) Eryazici, I.; Moorefield, C. N.; Newkome, G. R. *Chem. Rev.* **2008**, *108*, 1834−1895.
(23) Tam, A. Y. Y.; Wong, K. M. C.; Wang, G.; Yam, V. W. W. *Chem. Commun.* **2007**, 2028−2030.
(24) Zhao, L.; Wong, K. M.; Li, B.; Li, W.; Zhu, N.; Wu, L.; Yam, V. W. *Chem.—Eur. J.* **2010**, *16*, 6797−6809.
(25) Cai, X.; Liu, K.; Yan, J.; Zhang, H.; Hou, X.; Liu, Z.; Fang, Y. *Soft Matter* **2012**, *8*, 3756−3761.
(26) Zhang, J.; Guo, D. S.; Wang, L. H.; Wang, Z.; Liu, Y. *Soft Matter* **2011**, *7*, 1756−1762.
(27) Mecca, T.; Messina, G. M. L.; Marletta, G.; Cunsolo, F. *Chem. Commun.* **2013**, *49*, 2530−2532.
(28) Tam, A. Y.; Wong, K. M.; Yam, V. W. W. *J. Am. Chem. Soc.* **2009**, *131*, 6253−6260.
(29) Yam, V. W. W.; Wong, K. M.; Zhu, N. *J. Am. Chem. Soc.* **2002**, *124*, 6506−6507.
(30) Wong, K. M.; Yam, V. W. W. *Acc. Chem. Res.* **2011**, *44*, 424−434.
(31) McGuire, R., Jr.; McGuire, M. C.; McMillin, D. R. *Coord. Chem. Rev.* **2010**, *254*, 2574−2583.
(32) Tam, A. Y.; Wong, K. M.; Zhu, N.; Wang, G.; Yam, V. W. W. *Langmuir* **2009**, *25*, 8685−8695.
(33) Arena, G.; Calogero, G.; Campagna, S.; Monsù Scolaro, L.; Ricevuto, V.; Romeo, R. *Inorg. Chem.* **1998**, *37*, 2763−2769.
(34) Wadas, T. J.; Wang, Q.-M.; Kim, Y.-j.; Flaschenreim, C.; Blanton, T. N.; Eisenberg, R. *J. Am. Chem. Soc.* **2004**, *126*, 16841−16849.
(35) Birks, J. B.; Christophorou, L. G. *Proc. R. Soc. London, Ser. A* **1963**, *274*, 552−564.
(36) Birks, J. B.; Dyson, D. J. *Proc. R. Soc. London, Ser. A* **1963**, *275*, 135−148.
(37) Birks, J. B.; Christophorou, L. G. *Proc. R. Soc. London, Ser. A* **1964**, *277*, 571−582.
(38) Birks, J. B.; Lumb, M. D.; Munro, I. H. *Proc. R. Soc. London, Ser. A* **1964**, *280*, 289−297.
(39) Stevens, B.; Ban, M. I. *Trans. Faraday Soc.* **1964**, *60*, 1515−1523.
(40) Honda, C.; Katsumata, Y.; Yasutome, R.; Yamazaki, S.; Ishii, S.; Matsuoka, K.; Endo, K. *J. Photochem. Photobiol., A* **2006**, *182*, 151−157.
(41) Forster, L. S.; Rund, J. V.; Fucaloro, A. F. *J. Phys. Chem.* **1984**, *88*, 5012−5017.
(42) Chung, C. Y.; Yam, V. W. W. *J. Am. Chem. Soc.* **2011**, *133*, 18775−18784.